Micro- and Nanoscale Tensile Testing of Materials

D.S. Gianola and C. Eberl

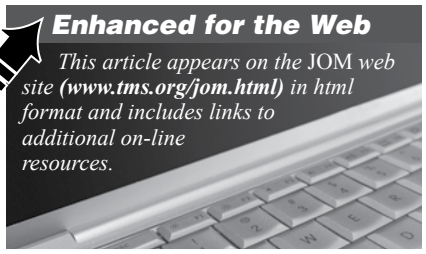

Enhanced for the Web

This article appears on the JOM *web site* ***(www.tms.org/jom.html)*** *in html format and includes links to additional on-line resources.*

This article reviews concepts and techniques for performing instrumented tensile testing of materials at small dimensions. State-of-the-art methods to probe tensile behavior of micro- and nanoscaled materials span many orders of magnitudes of force and displacement, often requiring a custom solution for each new material discovery. We discuss the experimental opportunities, challenges, and pitfalls in concert with the scientific insights revealed from tensile investigations at length scales where conventional wisdom is challenged on how materials deform.

INTRODUCTION

Developing mechanical tensile testing techniques and methodologies of materials in miniscule dimensions to accompany the accelerating pace of technological miniaturization has been a challenging task. Novel device architectures have been proposed that utilize tiny building blocks (e.g., hybrid materials, nanocomposites, microelectromechanical systems [MEMS] and nanoelectromechanical systems [NEMS] materials, nanostructured thin films, nanoporous structures, nanowires, and nanotubes) because of their superior properties, even in the absence of a complete understanding of the governing mechanisms for deformation. The race is on to uncover the mechanisms that give rise to different properties when atomic scales are approached and change our thinking on how materials deform. Yet, the accurate and reliable testing at these length scales is shrouded with uncertainty.

The following experimental questions arise: How can we fabricate small specimens with good geometric tolerances? How do we measure the dimensions of small samples that cannot be imaged with conventional optical methods? How can we measure and apply small forces with high dynamic range? How do we manipulate and grip small specimens?

This article focuses on instrumented small-scale tensile (i.e., stretching or pulling) testing approaches, where load is applied uniaxially and the resulting stress and strain state is nominally uniform in the specimen. Simply stated, micro- and nanotensile approaches differ in comparison to other small-scale methods in that the interpretation of data is relatively straightforward, while the technical hurdles can be high. Conversely, techniques such as nanoindentation are relatively simple to execute, while the interpretation can be challenging.

How would you…

…describe the overall significance of this paper?

In this paper we review state-of-the-art small-scale tensile testing techniques spanning several orders of magnitude of size and highlight exemplary case studies that have a significant impact on various subjects in materials science.

…describe this work to a materials science and engineering professional with no experience in your technical specialty?

As technology miniaturizes, we need new techniques to probe the mechanical response of materials at pertinent length scales. Some methods we can simply scale down in size, but at increasingly small scales when test specimens have dimensions smaller than the diameter of a human hair (~50 μm), we need radically new approaches. Here we review tensile techniques at the micro- and nanoscale.

…describe this work to a layperson?

Here, we discuss approaches to scale down tensile testing to probe mechanical properties of materials from the millimeter to the nanometer scale.

TENSILE TESTING APPROACHES AND TECHNIQUES

There are several experimental hurdles that must be overcome to do proper tensile testing of materials in order to obtain precise mechanical property measurements. In the macro-world, the majority of these issues has been studied in detail and in many cases standardized (e.g., ASTM standards). The pertinent questions at the micro- and nanoscale become: What techniques can we simply scale down from large-scale approaches, and at what point do we need radically different methodologies to deal with reduced dimensions? The following sections systematically address the steps necessary to realize a tensile test at small scales and highlight several unique approaches that researchers in the field have developed to overcome these challenges.

The synthesis of materials with reduced dimensions (e.g., coating materials, novel nanostructures, thin films) is a burgeoning field of research. Metrology for accurate sample measurement and micro- and nanostructural characterization must be juxtaposed with synthesis and testing. These topics are de-

serving of their own attention (see, for example, Reference 1), and major progress has been made in the last decades; advances have been made in marriage with the development of novel microscopy technologies. Here the emphasis will be placed entirely on the issues and challenges pertaining to mechanical testing of small-scale materials.

Specimen Harvesting, Manipulation, and Gripping

Specimens at the larger end of the length scales covered in this overview (envelope dimensions of several mm × hundreds of μm × tens to hundreds of μm, see, e.g., Figure 1) can be handled in much the same way that conventional tensile specimens are. Sharp tweezers can often be used for manipulating specimens, and more controlled air tweezers for soft and ductile specimens. In a recent review on microscale mechanical characterization, K.J. Hemker

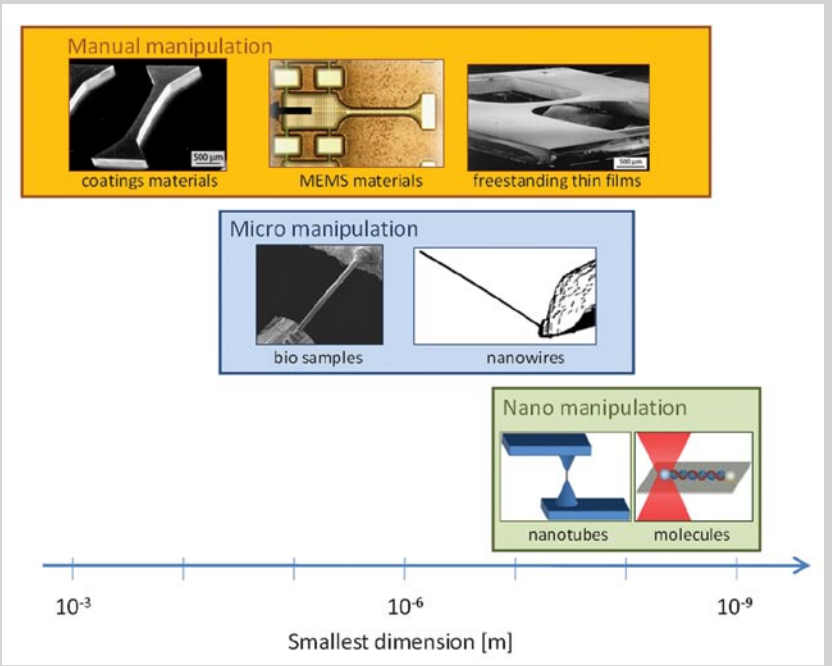

Figure 1. Specimen manipulation strategies are illustrated schematically across the length scales involved in micro- and nanotensile testing. The top row shows examples of specimens that can be handled using tweezers. The middle and bottom rows require manipulators to harvest and transfer specimens to a testing platform, and differ in the necessary motion fidelity. (LIGA Ni image reprinted, with permission, from the *Annual Review of Materials Research*, Volume 37 ©2007 by Annual Reviews. Thin film image reprinted with permission from SPIE.)

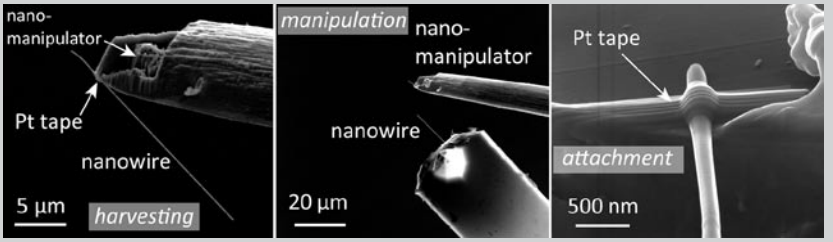

Figure 2. Scanning electron microscopy images showing strategies for harvesting, manipulating, and attaching quasi-1-D nanostructures. A nanomanipulator is operated in the SEM and can be attached to a specimen using local platinum deposition. Transfer and alignment can be accomplished by using the FIB to cut the specimen. A close-up view of platinum "tape" used for gripping during tensile testing, as deposited with the assistance of the e-beam.

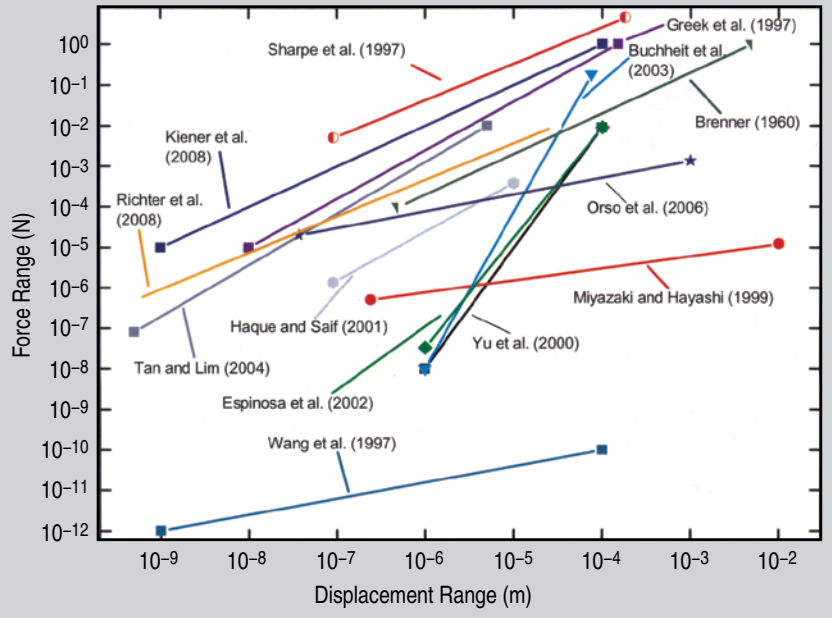

Figure 3. The force versus displacement range offered by a variety of small-scale tensile testing techniques, spanning approximately eight decades of force and displacement range.[21,30,40–43,50,60,85,92,111] The lower point represents the resolution of the system, while the upper point is the maximum allowable value. This plot gives guidelines for recommended testing approaches. (Figure courtesy of Steffen Orso.[44])

and W.N. Sharpe[2] highlighted techniques for fabricating and handling freestanding microspecimens and presented examples of the insightful results obtained from testing for a broad range of materials applications.

However, many micro- and nanoscale specimens are typically very fragile and cannot withstand the brutality of conventional handling tools (e.g., tweezers, hands). Two general categories of remedies are employed to accomplish specimen handling: mounting the specimen on a support structure that is large and/or stiff enough to handle easily with typical tools, and harvesting individual specimens from the location where they were grown, assembled, or dispersed using micro- and nanomanipulators and transferring them to a testing device. Figure 1 illustrates examples of specimen geometries as a function of size and manipulation scheme.

A support structure can easily be integrated into a microfabrication or MEMS processing scheme in order to test freestanding thin films. Both additive (e.g., deposition of layers on a substrate) and subtractive (e.g., etching through layers, removal of sacrificial layers) processes can be used in the process flow to implement a platform that consists of a thin film that is anchored to a substrate but released in the gage section. C.A. Neugebauer[3] developed such a method using gold films and a rock salt substrate as far back as 1960. D.T. Read and J.W. Dalley,[4] and later W.N. Sharpe, Jr. and colleagues,[5] extended this technique for testing films that are deposited on a silicon substrate. As shown in Figure 1, a freestanding polysilicon thin film specimen (3 μm thick) is framed by a silicon supporting structure consisting of 500 μm thick silicon grips and support strips on the periphery.[5] This die is handled easily with tweezers, and can be integrated into a tensile testing platform. Prior to testing, the support strips can be cut with a diamond-impregnated rotary tool so that the loads are only incurred by the thin film. This technique has been successfully utilized for the testing of Ti-Al-Ti,[4] polysilicon,[6] nanocrystalline aluminum,[7] gold,[8,9] SiN,[10] and SiC.[11]

An alternative method involves surface micromachining of thin-film materials on the surface of a substrate and subsequently removing sacrificial layers or etching below specimens to release the gage section, as introduced by T. Tsuchiya et al.[12] Figure 1 shows the so-called narrow thin-film specimen geometry of W.N. Sharpe et al.[13] One end of the specimen remains anchored to the substrate, while the other consists of a large paddle with arrays of patterned etch holes that allows for release from the substrate during etching. This paddle is attached to anchors that can be cut before testing using a sharp micromanipulator. The large paddle can be gripped electrostatically[12] or by gluing a stiff fiber and attaching the other end to a load cell.[13–17] One advantage of this method is the ability to test specimens in a more parallel fashion, since the alignment of the loading device needs to be accomplished only once per die. D.T. Read et al.[18] proposed an alternative paddle geometry that has been used by others[19,20] consisting of an annular ring on the free side of the specimen, allowing for a separate hook structure to apply forces to the specimen.

Co-fabrication of the specimen and testing apparatus has been proven to be an attractive strategy in situations where the materials synthesis can be integrated in the device process flow. This is particularly appealing for materials used in microelectronics, MEMS, and NEMS synthesized by vapor deposition methods, and allows for batch processing and testing of many specimens on a single wafer. Co-fabrication has the clear advantage of circumventing gripping and alignment issues by incorporating the specimen into the device fabrication using multiple photolithography masks, for example. M.A. Haque and M.T.A. Saif have co-fabricated and performed tensile testing of thin metal films as thin as 30 nm[21] and H.D. Espinosa and colleagues have employed this strategy to test polysilicon specimens and one-dimensional (1-D) nanostructures.[22]

The described strategies for specimen manipulation are not always feasible when a specimen's largest dimension is less than several tens of micrometers, as in the case of nanotubes, nanowires, nanobelts, and some biomaterials. Y. Zhu, C. Ke, and H.D. Espinosa[23] recently reviewed the state of the art of mechanical characterization of 1-D nanostructures, and point out that one of the largest challenges is the handling of extremely small specimens. Micro- and nanomanipulators can be used in conjunction with high-resolution imaging systems to locate, attach, transfer, and manipulate these structures to the desired testing platform. For example, several commercial nanomanipulators with multiple degrees of freedom are now available that make use of piezoelectric materials combined with so-called inertial drive mechanisms. These actuators exploit the difference between the static and dynamic coefficients of friction, offering sub-nanometer resolution with millimeter to centimeter ranges (examples of commercially available systems include Kleindiek Nanotechnik, Omniprobe, and Klocke Nanotechnik). By attaching fine tapered probes (typically sharpened by electropolishing, and many times re-sharpened by the focused ion beam [FIB]), tiny specimens can be manipulated and harvested with no to minimal handling damage. In situations where specimens can no longer be imaged using white-light optical microscopy, nanomanipulators can be integrated into transmission electron microscopy (TEM),[24,25] scanning electron microscopy (SEM), and/or FIB[26] environments where they can be used in conjunction with local deposition systems for specimen attachment.

Common approaches for in situ attachment include local deposition or accumulation of hydrocarbons present in the vacuum system using a focused e-beam (EBID),[27] or the local injection of a precursor gas (called a gas injection system, or GIS) that adsorbs to the sample surface and can be locally decomposed using EBID or an ion beam (IBID). The desired compound is deposited where the beam is scanned, and the reaction products are volatile and can be pumped away. This method has been utilized extensively,[28,29] and GIS systems currently exist with the capability of depositing gold, platinum, and tungsten. The GIS method has also been used for local metal deposition to grip specimens for tensile testing. For example, S. Orso et al. used IBID to deposit "fixation tape" of tungsten to individual setae from the leg of a beetle for subsequent tensile testing.[30] Figure 2 shows the manipulation and transfer of nanowires by utilizing a commercial nanomanipulator and

local platinum deposition. Limited information exists regarding the strength of these "tape" deposits given that the microstructure and corresponding properties vary wildly depending on the deposition conditions.[31] Nevertheless, this gripping method has proven to be sufficiently strong for specimens as large as several micrometers, generating forces as high as ~ 5 mN.[30]

In addition, the advent of atomic force microscopy (AFM/SPM) based techniques has spawned a new generation of tools using the atomically sharp tip as an end effector to manipulate objects as small as individual atoms.[32] This approach is often named the AFM nanorobot[33,34] and can be made more versatile by functionalizing the tip to enhance the specificity of binding to certain molecules or particles (often called chemical force microscopy). For example, S.H. Leuba et al. employed this approach to stretch single strands of chromatin and measured their mechanical response.[35]

Novel manipulation and patterning techniques have been proposed and could prove to be very useful for attachment of tensile specimens, particularly those that require high throughput or special environments (e.g., aqueous solutions, non-ambient conditions). Some examples include random dispersion of nanostructures in suspension solution onto patterned grids or by directed self-assembly to encourage pattern formation,[23] alignment using external electric fields by utilizing the dielectrophoresis effect,[36,37] and direct growth of nanostructures by patterning or manipulating growth catalyst particles in desired locations and orientations.[38,39] These methods show promise for accelerated tensile testing of materials to efficiently generate large materials properties datasets.

Actuation and Force/ Displacement Measurement

One must consider the expected forces and displacements that would be incurred when approaching micro- and nanoscale tensile testing (see Figure 3 for literature values of force and displacement ranges for a variety of testing approaches[40–44]). Other important considerations when choosing a testing apparatus are the materials properties that are desired (e.g., elastic moduli, yield strength, stress relaxation, etc.) and whether dynamic material changes (e.g., discrete deformation, yield points) are expected during testing. At larger scales, Sharpe, Hemker, and coworkers[2] showed that many microtensile testing needs can be satisfied using careful selection of commercially available components.

Actuation technologies exist that offer nanometer and sub-nanometer resolution, and others are available that offer large ranges of motion; the challenge is obtaining a system that provides high dynamic range (i.e., fine step sizes and large ranges). Piezoelectric actuators offer decided advantages in terms of resolution of motion (since the principle is based on atomic-level straining) and speed control, and can be fabricated in special stack geometries to extend the range of motion. However, piezo-based actuation systems are susceptible to direct current (DC) drift and stack designs are not always very compact, precluding use in restricted spaces (e.g., in situ experiments). High dynamic range actuators are commercially available that make use of the inertial drive mechanism mentioned previously, combining precision motion of piezoelectric materials with large travel (e.g., tens of millimeters). This motion can be accomplished using linear sliding or by a ratcheting motion of piezoelectric jaws over a finely threaded screw.

Thermal actuation has been demonstrated as a useful and stable actuation method,[45,46] which involves the coupling of electrical, thermal, and mechanical fields. A DC current is passed between external contacts connected to slender beams, which induces resistive heating along angled beams. The heat resulting from the Ohmic dissipation results in thermal expansion of the beams along their longitudinal axes and projects into rectilinear motion for actuation. The amount of force and displacement that the thermal actuator can generate is a function of the beam geometry, the angle of inclination relative to the actuation axis, the number of beams used, and the material properties of the actuator.

Once the actuation technique has been chosen, one must consider a method for measuring the tiny forces encountered in small-scale specimens. Many commercial load cells based on conventional technology such as Wheatstone bridges or internal leaf springs are available that provide the capability of measuring forces as small as several tens of micronewtons.

Flexure-based load measurement systems that rely on transverse deflection of beams perhaps offer the most versatility, since the load range can be customized to suit the testing needs simply by adjusting the geometry. This can be accomplished readily at larger scales by using CAD-based EDM or laser cutting methods, and by microfabrication or FIB milling at smaller length scales. Cantilevered beams are sensitive load sensors since they are very compliant; indeed, this point is exploited in AFM,[47] surface stress-induced chemical and biological sensing,[48] and stress evolution studies during thin-film growth.[49] For example, M.F. Yu et al.[50] used two opposing AFM cantilevers to manipulate and test multi-walled carbon nanotubes in tension. S. Gudlavaletti and colleagues[51] demonstrated the versatility of flexure-based systems by providing design considerations and constructing monolithic apparatuses to perform tensile testing at different length scales.

Several researchers promoted this technique for force measurement during tensile testing of one-dimensional nanostructures,[22,23,52] freestanding metallic thin films,[21,53] and polysilicon[22] by microfabricating testing devices that integrate actuators and load measurement devices all on a single chip. Haque and Saif[21] introduced an integrated testing device consisting of silicon beams and grips that are etched through the entire chip in order to perform in situ TEM tensile testing. They developed a new generation of testing platform,[54] as shown in Figure 4a, with some advantages including reference markers for relative displacement measurements (thus, 1-D strain) and the possibility for concurrent four-point electrical characterization. This device can be integrated easily into existing TEM straining holders and simple ex situ actuators, but requires external loading. Espinosa and co-workers[22] developed fully integrated testing platforms that rely on thermally driven actuators or capacitive structures inducing electrostatic forces (Figure 4b). Their devices require only that

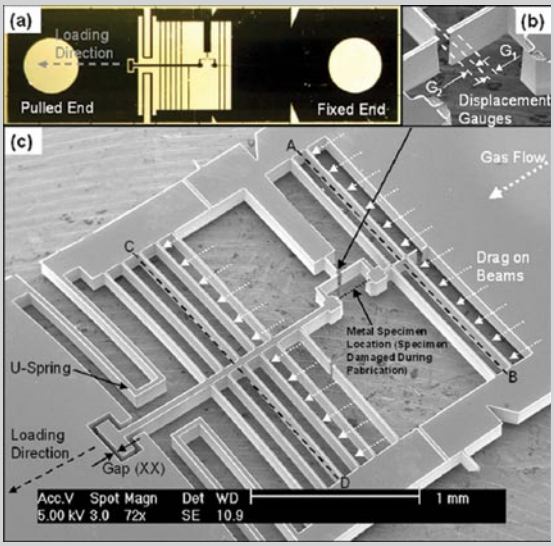

a

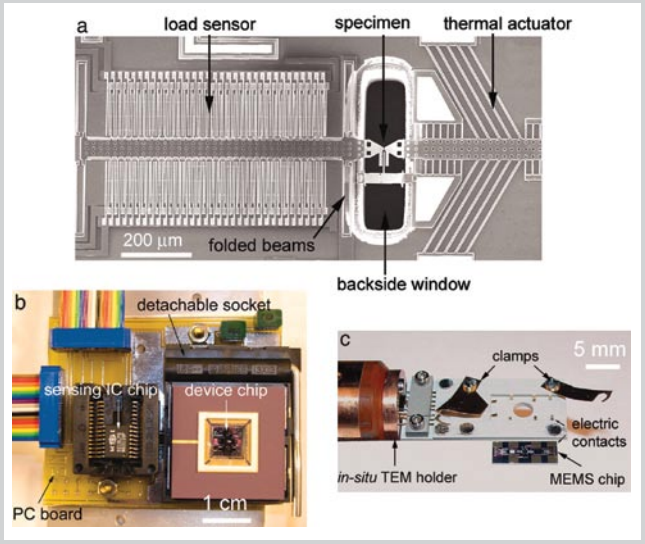

b

Figure 4. MEMS-based tensile testing platforms in which the specimen is co-fabricated with the testing apparatus. (a) Platform of Han and Saif,[54] which utilizes flexure beams for alignment and force measurement, and can be installed in in situ SEM or TEM straining holders. (Reused with permission from Jong H. Han, *Review of Scientific Instruments*, 77, 045102 (2006). Copyright 2006, American Institute of Physics.) (b) SEM image of platform of Espinosa et al.,[22] which has the actuator, load cell, and specimen all on-chip. Only external electrical connections are required to operate the device, and the device can also be operated in the TEM. (Copyright 2005 National Academy of Sciences, U.S.A.)

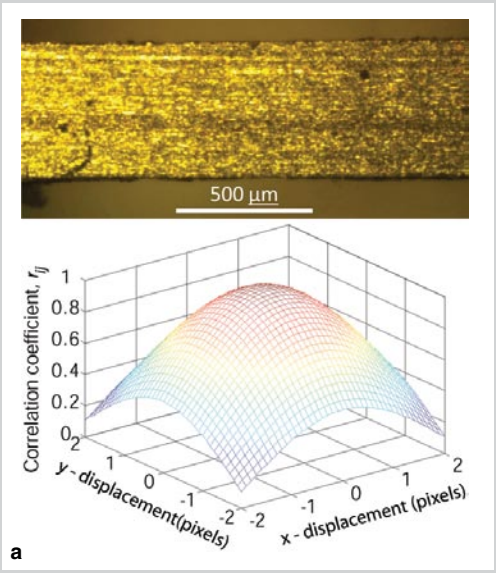

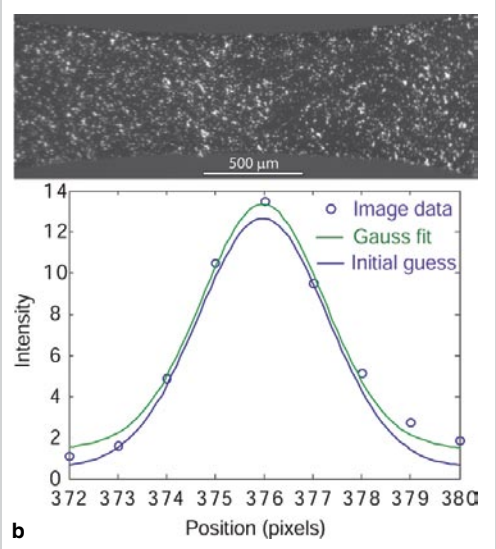

Figure 5. Examples of specimens with optimal contrast for (a) DIC and (b) DDIT non-contact strain measurement. (a) Image of a rolled Al 5053 microtensile specimen with natural surface contrast good for DIC, and corresponding correlation coefficient that is maximized during DIC procedure. (b) Image of surface of nanocrystalline aluminum submicrometer thin film decorated with SiOx particles, ideal for DDIT. A section of one particle shown as the intensity from the digital camera as a function of position. A Gauss function is fit to the raw data, and the evolution of the peak center can be tracked with sub-pixel resolution.

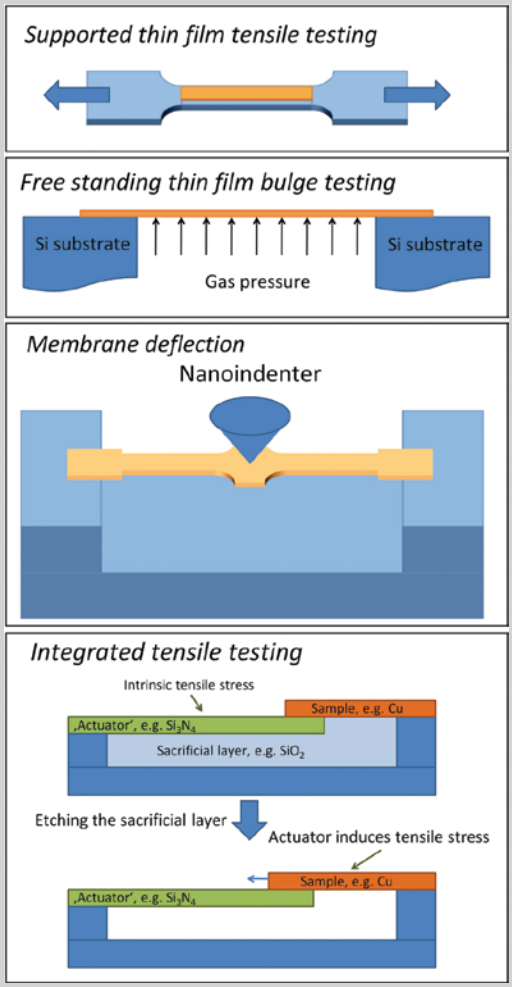

Figure 6. Examples of alternative small scale testing devices that lead to tensile stresses and strains in specimens: thin film deposited on a polymer dogbone, bulge testing of freestanding thin film, membrane deflection technique using a nanoindenter system to stretch thin films, and use of intrinsic stress in SiNx actuators in a microfabrication process flow. Subsequent etching of a sacrificial layer causes the SiNx beam to pull on the testing specimen.

electrical contacts be made to the device, which can be easily accomplished using standard wire bonding. R.S. Ruoff et al.[55] designed and implemented a flexure-based, microfabrication-realized testing platform with a novel geometry that produces displacement de-amplification from thermal actuators, resulting in precise nanometer-level control.

Nanoindentation systems are most often utilized for compression testing of materials (e.g., sharp indentation, pillar compression), but can also be utilized for small-scale tensile testing.[52] Some transducer designs rely on electromagnets for force actuation and capacitive systems for displacement measurement (see for example Reference 56 for a review on instrumented indentation), while others utilize electrostatic interactions between capacitive structures for force generation.[57] The latter systems employ a three-plate capacitor design and superimpose high-frequency antiphase alternating current (AC) signals to opposing capacitor plates to measure displacement.[57] It should be noted that both transducer designs are inherently force-controlled, but sophisticated feedback systems can be used to achieve quasi-displacement control during testing.

Focused light can also be used to apply or measure forces on small specimens. The research group of C. Bustamante[58] implemented an optical trapping system (also known as optical tweezers) to experimentally investigate the extensibility of DNA. This approach exploits the electrical field gradient produced by a focused laser beam, which interacts with and traps dielectric particles (typically glass or polymeric beads attached to biomolecules) in the center of the beam. If the bead is moved from the optical center, then a restoring force is applied to the dielectric particle due to the momentum transfer from the scattering of light, allowing for mechanical testing experiments. Position-sensitive detectors (e.g., photodiodes or CCD cameras) are placed downstream from the optical path and can detect beam displacements (at the nanometer level), while forces (as low as 10^{-13} N) are applied by either steering the beam or by precisely moving the other end of the specimen using a piezoelectric stage.[59] It should be noted that careful and tedious calibration of these systems is necessary to quantify the changing trap stiffness and displacement output.[60]

Strain Measurement

Accurate tensile testing requires direct strain measurement in the gage section[61] of the specimen and in small-scale testing this can be achieved by non-contact strain measurement methods. Notable approaches include the interferometric strain displacement gage (ISDG[62]), tracking of diffraction spots from gratings deposited on specimen surfaces,[63] digital image correlation (DIC),[16,64] and differential digital image tracking (DDIT).[15,30] These techniques also allow for the measurement of the lateral strain to measure Poisson's ratio.[5,65] Digital image correlation and DDIT have the advantage of full-field capability giving local fidelity (e.g., strain heterogeneities near grain boundaries).[66] These techniques measure the strain even after tensile necking extending the measureable stress-strain behavior beyond the maximum engineering stress.[65] In the case of in situ tensile testing, DIC and DDIT are ideal methods for strain measurement, as the SEM,[66–68] FIB,[30] or AFM[16] can be used as image sources during the test. Thus, quantitative information can be extracted in addition to imaging the deformation mor-

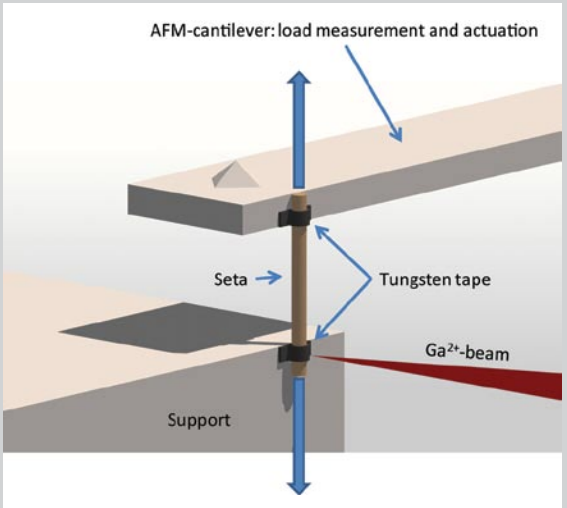

a

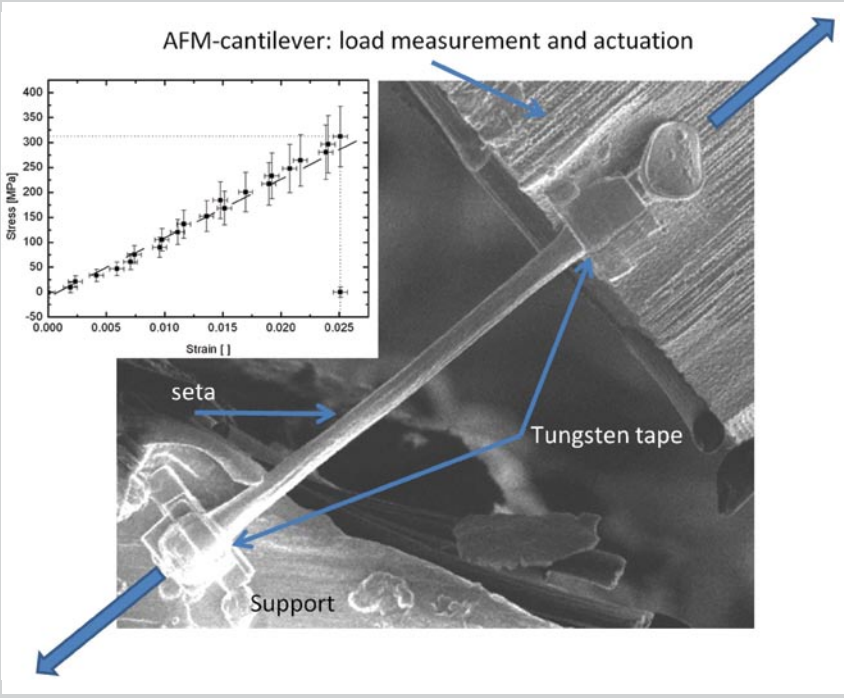

b

Figure 7. In situ FIB tensile testing approach for individual seta from the leg of a beetle. (a) Illustration showing AFM cantilever load measurement device, specimen, and attachment points. (b) FIB image of a specimen during testing. Inset shows stress strain behavior. Strain was measured locally using DDIT of captured images.

phology during testing.

The basic premise of DIC is as follows, and a representative image demonstrating good surface contrast on a microspecimen is shown in Figure 5a. The correlation coefficients of subsets of consecutive images (typically between 10×10 to 40×40 pixels^2) are calculated and plotted versus their position. Biquadratic functions, for instance, can be used to locate the maximum correlation coefficient (with sub-pixel resolution) that is representative of the optimal fit between the subsets of the two images (Figure 5a). Differential digital image tracking requires intensity peaks in the source images that can be tracked by a peak fitting algorithm (Figure 5b). This method can achieve a resolution of up to a thousandth of a pixel, which allows for good strain fidelity even in the absence of many pixels (e.g., AFM images with ~200×200 pixels^2 resulting in strain resolutions of up to $\Delta\varepsilon = 10^{-5}$). Ultimately, the resolution of DIC and DDIT primarily hinge on the noise present in the imaging system. Differential digital image tracking is typically less susceptible to local image noise since features are tracked that span multiple pixels. Free MATLAB® code for DIC and DDIT is available online.[69]

Indirect Tensile Testing Methods

The focus of this paper is on instrumented tensile testing in which the uniaxial load and displacement are measured directly and independently. However, several small-scale testing methods have been reported that induce tensile loads in specimens and are capable of measuring full stress-strain curves. Notable examples include plane-strain bulge testing,[70] the membrane deflection technique,[71] and an on-chip residual stress-induced actuation method.[72] These methods are illustrated in Figure 6.

Co-deforming a thin film with a polymer substrate (Figure 6) is another way to stabilize fragile specimens and is also of technological interest for use in flexible electronics for displays and active textiles. Several researchers have utilized this approach to study the tensile behavior of films as thin as 20 nm.[73–77] Furthermore, in situ x-ray diffraction can be used to quantify stress evolution in crystalline materials since the total force cannot be directly related to stress in the thin film. Upon analyzing the diffraction patterns, one can calculate the elastic multi-dimensional lattice strains from interplanar crystalline spacings and combining multiple measurements in orientation space. These quantities can be related via careful analysis to the stress in the crystal via the elastic constants.[78,79] The influence of Poisson contraction and time-dependent relaxation of the underlying polymer can therefore be mitigated as employed extensively by H. Hommel and O. Kraft,[73] P.A. Gruber et al.[80,81] for continuous films and S. Olliges et al. for structured films.[82]

Bulge testing involves pressurizing a freestanding thin film that is clamped at its edges to induce tensile stresses in the membrane (Figure 6); the pressure and deflection of the membrane are measured independently, as introduced by J.J. Vlassak and W.D. Nix.[70] This has been applied to the testing of various metal films with and without passivation layers.[83,84]

The membrane deflection technique was developed by H.D. Espinosa and colleagues,[71,85] where a long doubly clamped freestanding thin film is pushed in its center using a nanoindenter (Figure 6). Given the lack of bending stiffness in thin films, the transverse loading translates to tension in the membranes on either side of the loading point. Force is measured by the nanoindenter,

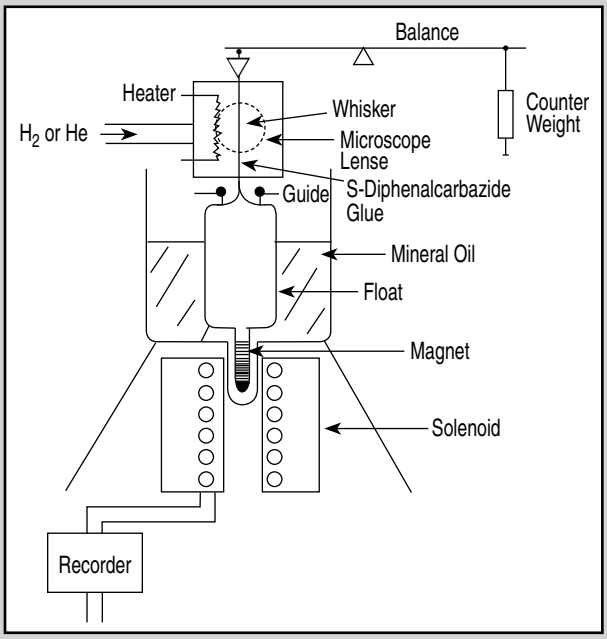

a

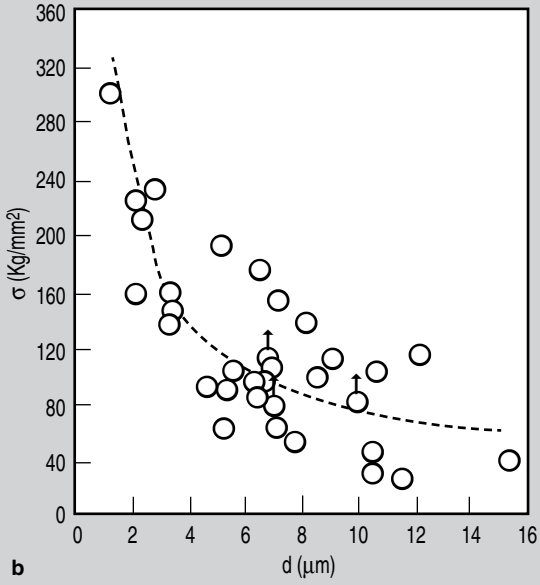

b

Figure 8. Tensile testing of single crystalline metallic microwhiskers.[92] (a) Experimental tensile testing constructed by Brenner and (b) results of copper whisker fracture strength as a function of whisker size, showing clear size dependence. (Reused with permission from S.S. Brenner, *Journal of Applied Physics*, 27, 1484 (1956). Copyright 1956, American Institute of Physics.)

and the vertical deflection can be measured using an interferometer.

Lastly, N. André et al.[72] developed a tensile testing technique which can be integrated into a MEMS or microelectronics process, where the actuation is carried out by residual stresses in SiN_x. During etching of a sacrificial layer that initially holds the layers in place, the intrinsic stress in the SiN_x actuator pulls on the sample as illustrated in Figure 6, and by integrating several of these structures with different actuator lengths, the actuated displacement can be varied. The load on the sample can be measured by the difference in displacement of each actuator compared to a stress-free state. Each actuator-sample structure represents one data point on the stress-strain curve.

INSIGHTS GAINED FROM SMALL-SCALE TENSILE TESTING

Micro- and nanotensile testing have helped further our understanding of how small volumes of materials deform, as shown in the following examples.

Tensile Testing of Biological Attachment Devices

Biologically inspired adhesion systems have recently attracted significant attention as a replacement for chemistry-based adhesives, tapes, and industrial grippers. Some insects and geckos use hierarchical hairy attachment systems of brush-like structures as small as 200 nm to reversibly adhere to walls and chase down their prey. Several researchers have shown that van der Waals interactions and capillary forces provide the observed adhesion[86–89] and have studied the related scaling laws. The findings can be used to identify the optimum geometric and materials properties via adhesion maps.[90,91] Measurements of the mechanical properties of these small structures is necessary for efficient design yet challenging, as the diameters of setae scale from several micrometers down to 200 nm with lengths between several micrometers and 100 μm.

Orso et al.[30] were successful in utilizing a micromanipulator mounted into an FIB microscope to separate, cut, and fix single setae from the leg of a gastrophysa viridula (beetle) and carry out in-situ microtensile tests. The experimental setup for tensile testing is shown in Figure 7. The load was measured by an AFM tip attached to the micromanipulator and the setae were glued by tungsten tapes deposited using IBID to a metal block and the AFM tip. The strain was calculated using DDIT from the FIB micrographs obtained continuously throughout the test.

The measured Young's modulus of the gastrophysa viridula setae was 13.3 ±1 GPa and the reported ultimate strength was 310 ± 60 MPa. The mechanical behavior showed almost ideal elastic behavior (inset of Figure 7) and compares with properties of chitin fiber-reinforced composite materials. The authors pointed out that the Young's modulus of biological materials is often higher in vacuum than under normal atmospheres due to dehydration. This study set a precedent for extracting the properties of biological attachment systems, which aids designers in selecting bio-mimicking materials and optimizing structural design for the development of artificial attachment systems.

Size-Dependent Plastic Behavior in Single-Crystalline Metals

More than fifty years ago, S.S. Brenner[92] published seminal work on the deformation of microscale single crystals to convincingly demonstrate that size indeed does matter, and deformation behavior of metals can be altered by simply changing the external specimen size. He reported tensile testing results of copper, iron, and silver whiskers ranging in diameter from approximately 1 μm to 15 μm and 1 mm to 4 mm in length that were grown using reduction of halides and tested in the apparatus shown in Figure 8a. Stress-strain behavior was characterized as strong, but with limited plastic flow, and pronounced deviations from linear elasticity were measured in the iron whiskers that were attributed to strains that exceeded the linear elastic limit of Hookian elasticity.[92] He showed that the ultimate strength of the whiskers showed prominent size dependence (Figure 8b), with critical resolved shear strengths falling closely to the lower estimate for the ideal strength of these metals in the case of the smallest whiskers.

Brenner followed up this work[93,94] with more results on copper, silver, and gold whiskers using a modified setup that prevented the load train from exhibiting large deflections at the point of a large excursion event. This improvement allowed for the elucidation of sharp yield points, followed by regions of "easy glide" at a fraction of the yield point stress (as little as 10%) that was characterized by Lüders band propagation. Interestingly, the yield point exhibited size dependence, while the lower flow region did not. These observations, coupled with experiments that showed that a fractured whisker with less volume could be re-tested to recoup an even higher yield point, indicated that these whiskers had minimal starting defects and extreme stresses were required to nucleate defects. The nucleation stress was dependent on the probability of finding a critical defect of a critical size; thus, the measured volume or surface area dependence, akin to the classic experiments on the deformation of glass rods.[95] The results of this work highlighted the importance of discrete defects in small volumes, catalyzing the mantra of "smaller is stronger," a departure from our conventional wisdom of continuum descriptions of plasticity.

Recently, micro- and nanocompression has been developed by M.D. Uchic and colleagues[96,97] to study size-dependent (e.g., intrinsic and extrinsic size effects) and site-specific (e.g., local properties of composites, multi-phase materials, etc.) properties of materials, as discussed in a companion paper in this issue. This approach makes use of an FIB to fabricate small structures with control of size, and experimental studies on the deformation of face-centered cubic (fcc),[96,98–102] body-centered cubic (bcc),[103,104] and amorphous metals[105–107] have been conducted. Crystalline metals have shown a clear size dependence on the yield or flow stress. A vigorous debate has taken place to explain the underlying deformation mechanisms responsible for the size effect and departure from bulk behavior that have been revealed by this technique. The prevailing mechanistic explanations for fcc materials invoke the importance of dislocation source nucleation and activation,[99] source truncation by free

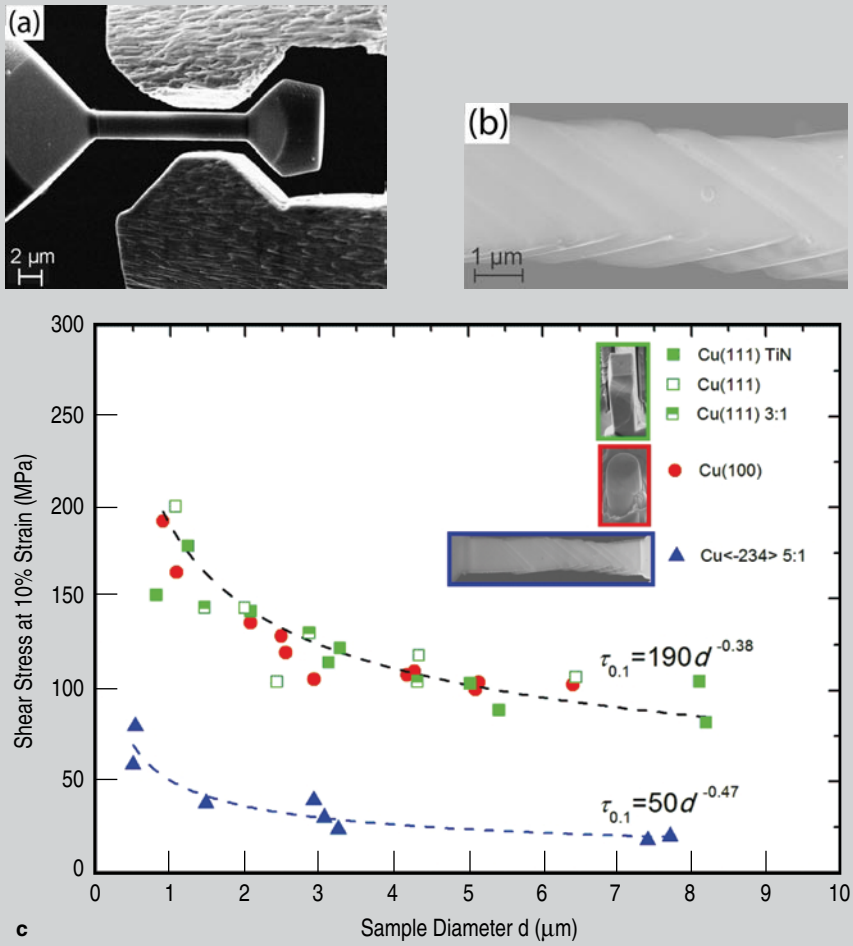

Figure 9. In situ SEM tensile testing of FIB fabricated single-crystalline microtensile specimens.[111] (a) The specimen and the grip are fashioned using the FIB to carve a gage section and a negative mold for gripping. (b) Deformed tensile specimens with sizes ranging from 0.5 to 8 μm demonstrated discrete slip band formation on the surfaces. (Reprinted from Reference 111 with permission from Elsevier.) (c) Resolved shear stress at 10% strain vs. sample diameter, showing distinct strengths and scaling depending on the deformation constraint, imposed by either testing in compression or changing the aspect ratio of the specimen.[110] (Reprinted from Reference 110 with permission from Elsevier.)

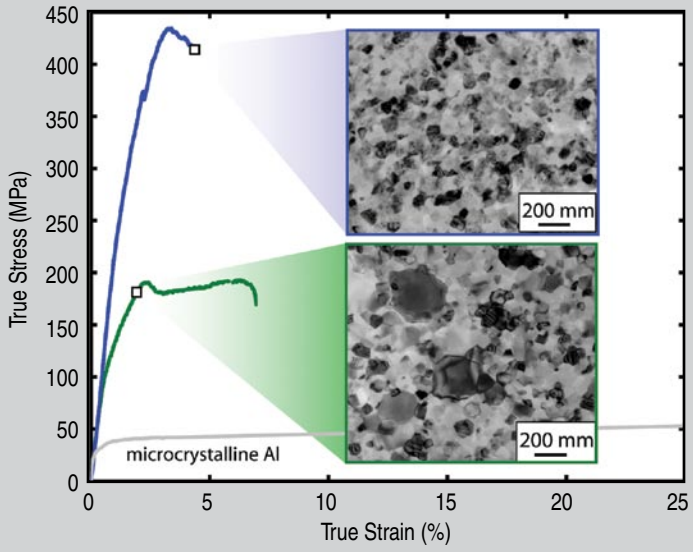

Figure 10. Microtensile stress-strain curves for submicrometer nanocrystalline aluminum thin films showing two distinct behaviors.[7] The curve with the highest strength, gradual deviation from plasticity, and limited ductility is representative of a specimen that maintains its nanocrystalline grain size. By contrast, specimens observed to undergo stress-assisted room-temperature grain growth exhibit lower yield strengths and regions of extended plasticity.

surfaces and subsequent exhaustion,[108] and dislocation starvation of defect-free crystals.[109] These compression experiments have revealed significant insight on the deformation of small metallic volumes, but the effect of the compressive loading modality (e.g., heterogeneous stress state from column tapering, stress concentrations arising from friction between the punch and the specimen, poorly defined boundary conditions) on the observed size effect is still elusive.

Recently, D. Kiener and colleagues[110,111] and Uchic et al.[97] developed in situ SEM methods for tensile testing of single-crystalline metallic specimens fabricated using FIB methods. The specimen and gripping configuration from Kiener et al. is shown in Figure 9, and was used for tensile specimens with sizes ranging from 0.5 μm to 8 μm. The major finding of this work is that tensile specimens with aspect ratios (length to width ratio) of 2:1 or higher exhibited yield strengths that were approximately three times lower than equivalent compression experiments using the same FIB parameters and experimental testing apparatus (Figure 9c). An extension of this work[110] demonstrated that reversing the loading of a tensile specimen into compression does not alter the yield strength; no tension-compression asymmetry was measured in these specimens. However, lowering the aspect ratio of the tensile specimens to mimic that of the compression pillars returns the strength to that measured from compression. Moreover, pronounced hardening is measured for low-aspect-ratio specimens. This point is attributed to the interaction and constraint of dislocation glide planes with the boundaries of the specimen, which will induce dislocation pile-ups leading to measurable hardening and a size dependence of the strength. Taken as a whole, these experiments emphasize the importance of boundary conditions, particularly in single-crystal deformation, and inspire the need to deconvolute the role of testing artifacts from intrinsic size-dependent response.

A bridge between the experiments of Brenner and the micro- and nanocompression and microtension experiments of specimens fabricated using the FIB is still missing, given that microwhiskers

demonstrated strengths close to the ideal strength while similarly sized specimens fabricated using the FIB show strengths significantly far away from this upper bound. Recent experiments from H. Bei and colleagues[112] provide evidence to suggest that the difference in measured strength lies primarily on the pre-existing defect structures in the material. In those works, molybdenum alloy compression pillars were fabricated by directional solidification of a eutectic and subsequent etching of the matrix, and no use of the FIB was needed. These pillars were presumably defect-free and demonstrated strengths near the calculated theoretical strength of molybdenum and no size dependence was measured. Size-dependent behavior and lower strengths returned when these specimens were irradiated with the FIB using conditions that emulate pillar preparation,[113] or when the composite material was pre-strained prior to etching and testing of the molybdenum alloy pillars.[114] Recent experiments by G. Richter et al.[52] reporting tensile testing of defect-free copper nanowhiskers complement the experiments of Bei and Brenner, also show a departure from pillar behavior, and give strengths at or near the ideal strength. The emerging picture suggests that the presence or absence of pre-existing defects in small volumes greatly contributes to the measured mechanical response of the material, and points to the need for thorough nanostructural characterization to accurately predict deformation and strength.

Deformation Mechanisms in Nanocrystalline Metals

Small-scale tensile testing has also made significant gains toward the understanding of deformation behavior of nanocrystalline metals, where the internal length scale given by the grain size defines the mechanical response. It is now generally accepted that nanocrystalline metals exhibit high strength and limited ductility in comparison with their coarse-grained counterparts, and conventional dislocation descriptions of crystal plasticity are abated when the grain size is reduced below approximately 100 nm. Elucidating the new mechanisms to accommodate plasticity that take over at reduced length scales has been the subject of vigorous research activity, along with several reviews (see, for example References 115–117). Proposed mechanisms that contribute to measurable global plastic strains include partial dislocation emission and subsequent absorption from grain boundaries, deformation twinning, grain boundary sliding, enhanced grain boundary diffusion, and grain boundary migration. The common denominator in all of these processes is that the large fraction of interfaces plays a large role in governing deformation.

Microtensile testing has been instrumental in characterizing the mechanical behavior of nanocrystalline metals,[118–120] primarily since large, fully dense volumes of these materials are difficult to synthesize, thus precluding the use of conventional tensile testing. For example, microtensile testing coupled with post-mortem TEM[118] and in situ x-ray diffraction[119] revealed that plastic deformation in nanocrystalline aluminum and nickel does not leave stored dislocation content in the interior of the grain as one would expect in microcrystalline materials. These studies helped form the currently accepted wisdom that grain boundaries serve as both the source and sink for dislocations in nanocrystalline metals.

In parallel, nanostructured materials are encountered in many thin film, MEMS, and NEMS applications, as the film deposition methods often synthesize material with nanoscaled grains. Freestanding thin film microtensile testing has been employed to measure yield strength, elastic moduli, hardening, and ductility of vapor-deposited nanocrystalline materials.[7,63] Room-temperature mechanical characterization of freestanding submicrometer aluminum thin films with thicknesses between 100 nm and 400 nm by D.S. Gianola and colleagues[7,65,121] have demonstrated that nanostructures can be unstable under the influence of stress, even those that demonstrate good thermal stability. Two general classes of deformation were uncovered as shown in Figure 10, briefly characterized as either strong with limited ductility and a stable microstructure or intermediate strengths with "extended" ductility and an evolving microstructure. The occurrence of stress-driven high-angle grain boundary migration was correlated to the content of impurities present during deposition.[122] Characteristics of the growth were not commensurate with conventional descriptions of grain growth[123] and instead appear to be in line with the notion of shear stress-driven coupled motion of both high- and low-angle grain boundaries, as postulated by J.W. Cahn and co-workers.[124,125]

CONCLUSIONS

Tensile testing at small size scales is an attractive field of research and technology since the output is directly interpretable, without recourse to complex models. Experimental techniques have advanced and become commercially available, enabling instrumented testing in an increasingly controlled manner. The most important developments are the availability of easy-to-use non-contact strain measurements and small scale actuators and transducers, combined with sensors of high fidelity and dynamic range.

Ultimately, engineers of all disciplines want predictive models of physical phenomena. Extracting materials properties across the length scale spectrum will give us physically based and technologically relevant models. Understanding the fundamental response of the building blocks of complex systems, coupled with a good understanding of physical constraints, will allow for the possibility of true predictive capability and intelligent engineering design. Equipped with the hierarchical knowledge of deformation at all length scales, one can push the limits of materials properties space[126] by synergistically combining materials behavior in a hybrid manner.

OUTLOOK

While the design of small-scale applications can often be based solely on elastic and plastic properties drawn from tensile testing, requirements during lifetime will be multi-faceted and lifetime can only be predicted if we understand the physical mechanisms at all scales. The various stimuli are inherently coupled and the materials properties should be measured in environments that emulate real use (e.g., integrated circuits, photovoltaics, fuel cells, advanced batteries). Short diffusion paths,

multiaxial stress states, cyclic loading, and elevated temperature have distinct implications at different length scales and generate the need for intensive investigations. Fatigue in pure thin films has been under investigation for some time now[127–129] and studies have found that thinner films can show higher lifetimes, which is a promising result. Tensile testing at elevated temperature is still limited although MEMS materials have been tested,[130] but reliable temperature control is still challenging and new concepts are needed if one desires creep testing. Advancements in coupled mechanical measurements techniques (e.g., coupled with thermal, electrical, photonic, or chemical loads) at small length scales are promising and represent an exciting arena for research. Transient tests do offer the opportunity to probe thermally activated processes and can generate new insights on active defect mechanisms.

Round-robin tensile tests, in which multiple laboratories with distinct testing capabilities collaboratively test batches of specimens to interrogate the uncertainty of measurement techniques, offer a possibility to formulate testing protocols and standardization. Tensile techniques at decreasingly small scales are still in development stages, but the ultimate goal should be to achieve testing standards commensurate with those at larger scales. Research laboratories should unite to ensure reliable and repeatable results.

Many systematic small-scale tensile testing studies have converged to the following answer: The elastic properties of fully dense microspecimens are similar to those of their bulk counterparts, as long as the effects of texture, anisotropy, and porosity are properly accounted for (see, for example, polysilicon used in MEMS[2]). Conclusive experimental evidence that demonstrates the effects of surface stress on both the elastic and plastic properties of materials with nanometer dimensions is elusive. Careful and systematic tensile testing can offer significant insight here and represents a direct way of measuring such effects.

ACKNOWLEDGEMENTS

The authors would like to thank the cast of characters that inspired their interest in small-scale mechanical testing; in particular our mentors Kevin J. Hemker and William N. Sharpe, Jr., from whom we learned the science and art of microtensile testing. C.E. would like to acknowledge financial support from the Deutsche Forschungsgemeinschaft. D.S.G. acknowledges support from an Alexander von Humboldt Postdoctoral Fellowship.

References

1. Y. Gogotsi, editor, *Nanomaterials Handbook* (Oxford, U.K.: Taylor and Francis, Inc., 2006).
2. K.J. Hemker and W.N. Sharpe, *Annual Review of Materials Research*, 37 (1) (2007), pp. 93–126.
3. C.A. Neugebauer, *Journal of Applied Physics*, 31 (6) (1960), pp. 1096–1101.
4. James W. Dally and David T. Read, *JMR*, 8 (1993), pp. 1542–1549.
5. W.N. Sharpe, Jr. et al., *Micro Electro Mechanical Systems, 1997 (MEMS '97)* (Piscataway, NJ: IEEE, 1997), pp. 424–429.
6. K.J. Hemker et al., *Journal of Microelectromechanical Systems*, 10 (3) (2001), pp. 317–326.
7. D.S. Gianola et al., *Acta Materialia*, 54 (8) (2006), pp. 2253–2263.
8. R.D. Emery and G.L. Povirk, *Acta Materialia*, 51 (7) (2003), pp. 2067–2078.
9. W.N. Sharpe et al., unpublished work (2008).
10. R.L. Edwards, G. Coles, and W.N. Sharpe, Jr., *Experimental Mechanics*, 44 (1) (2004), pp. 49–54.
11. C.A. Zorman et al., *Journal of Microelectromechanical Systems*, 14 (4) (2005), pp. 664–672.
12. T. Tsuchiya et al., *Micro Electro Mechanical Systems, 1997 (MEMS '97)* (Piscataway, NJ: IEEE, 1997), pp. 529–534.
13. W.N. Sharpe, K.T. Turner, and R.L. Edwards, *Experimental Mechanics*, 39 (3) (1999), pp. 162–170.
14. W.N. Sharpe et al., *Proceedings of IMECE 2006, 2006 ASME International Mechanical Engineering Congress and Exposition* (New York: ASME, 2006), p. 13290.
15. W.N. Sharpe et al., *Experimental Mechanics*, 47 (5) (2006), pp. 649–658.
16. Ioannis Chasiotis and Wolfgang Knauss, *Experimental Mechanics*, 42 (1) (2002), pp. 51–57.
17. S.A.I. Johansson and S. Greek, *Micromachined Devices and Components III, V*olume 3224 (Bellingham, WA, SPIE, 1997), pp. 344–351.
18. D.T. Read et al., *Scripta Materialia*, 45 (5) (2001), pp. 583–589.
19. G. Coles et al., *Mechanical Properties of Structural Films,* ed. C.L. Muhlsteom and S.B. Brown (West Conshohocken, PA: ASTM, 2001), pp. 3–15.
20. B.L. Boyce et al., *Journal of Microelectromechanical Systems*, 16 (2) (2007), pp. 179–190.
21. M.A. Haque and M.T.A. Saif, *Scripta Materialia*, 47 (12) (2002), pp. 863–867.
22. Y. Zhu and H.D. Espinosa, *Proceedings of the National Academy of Sciences of the United States of America*, 102 (41) (2005), pp. 14503–14508.
23. Y. Zhu, C. Ke, and H.D. Espinosa, *Experimental Mechanics*, 47 (1) (2007), pp. 7–24.
24. J. Cumings and A. Zettl, *Science*, 289 (5479) (2000), pp. 602–604.
25. P. Poncharal et al., *Science*, 283 (5407) (1999), pp. 1513–1516.
26. P.A. Williams et al., *Applied Physics Letters*, 80 (14) (2002), pp. 2574–2576.
27. H.W.P. Koops et al., *Japanese Journal of Applied Physics Part 1-Regular Papers Short Notes & Review Papers*, 33 (12B) (1994), pp. 7099–7107.
28. F.A. Stevie and L.A. Giannuzzi, editors, *Introduction to Focused Ion Beams: Instrumentation, Theory, Techniques and Practice* (New York: Springer, 2005).
29. C.A. Volkert and A.M. Minor, *MRS Bulletin*, 32 (5) (2007), pp. 389–395.
30. S. Orso et al., *Advanced Materials*, 18 (7) (2006), pp. 874–877.
31. H. Hiroshima et al., *Japanese Journal of Applied Physics Part 1-Regular Papers Short Notes & Review Papers*, 38 (12B) (1999), pp. 7135–7139.
32. D.M. Eigler and E.K. Schweizer, *Nature*, 344 (6266) (1990), pp. 524–526.
33. D. Nyyssonen, L. Landstein, and E. Coombs, *Journal of Vacuum Science & Technology B*, 9 (6) (1991), pp. 3612–3616.
34. M. Sitti and H. Hashimoto, *Advanced Robotics*, 13 (4) (1999), pp. 417–436.
35. M.A. Karymov et al., *Single Molecules*, 1 (2) (2000), pp. 185–192.
36. Yu Huang et al., *Science*, 291 (5504) (2001), pp. 630–633.
37. D.L. Fan et al., *Applied Physics Letters*, 85 (18) (2004), pp. 4175–4177.
38. Jing Kong et al., *Nature*, 395 (6705) (1998), pp. 878–881.
39. R. He et al., *Advanced Materials*, 17 (2005), pp. 2098–2102.
40. T.E. Buchheit et al., *Journal of Materials Science*, 38 (20) (2003), pp. 4081–4086.
41. W.N. Sharpe, B. Yuan, and R.L. Edwards, *Journal of Microelectromechanical Systems*, 6 (3) (1997), pp. 193–198.
42. E.P.S. Tan and C.T. Lim, *Review of Scientific Instruments*, 75 (8) (2004), pp. 2581–2585.
43. Hiroshi Miyazaki and Kozaburo Hayashi, *Biomedical Microdevices*, 2 (2) (1999), pp. 151–157.
44. S. Orso, "Structural and Mechanical Investigations of Biological Materials using a Focused Ion Beam Microscope" (Ph.D. thesis, Universität Stuttgart, 2005).
45. H.D. Espinosa, Y. Zhu, and A. Corigliano, *J. Micromech. Microeng.*, 16 (2006), pp. 242–253.
46. A.A. Geisberger et al., *Journal of Microelectromechanical Systems,* 12 (4) (2003), pp. 513–523.
47. G. Binnig, C.F. Quate, and Ch. Gerber, *Phys. Rev. Lett.*, 56 (9) (1986), pp. 930–933.
48. V. Nickolayet al., *Review of Scientific Instruments*, 75 (7) (2004), pp. 2229–2253.
49. K. Kinosita et al., *Japanese Journal of Applied Physics*, 6 (1967), pp. 42–53.
50. M.F. Yu et al., *Science*, 287 (5453) (2000), pp. 637–640.
51. S. Gudlavalleti, B. Gearing, and L. Anand, *Experimental Mechanics*, 45 (5) (2005), pp. 412–419.
52. G. Richter et al., "Ultra High Strength Single Crystalline Nano-Whiskers Grown by Physical Vapour Deposition" (unpublished work, 2009).
53. M.A. Haque and M.T.A. Saif, *Proceedings of the National Academy of Sciences of the United States of America*, 101 (17) (2004), pp. 6335–6340.
54. J.H. Han and M.T.A. Saif, *Review of Scientific Instruments*, 77 (4) (2006), DOI:10.1063/1.2188368 .
55. Shaoning Lu et al., *Review of Scientific Instruments*, 75 (6) (2004), pp. 2154–2162.
56. S. Rajagopalan and R. Vaidyanathan, *JOM*, 54 (9) (2002), pp. 45–48.
57. B. Bhushan et al., *Philosophical Magazine A*, 74 (1996), pp. 1117–1128.
58. S.B. Smith, Y.J. Cui, and C. Bustamante, *Science*, 271 (5250) (1966), pp. 795–799.
59. D.G. Grier, *Nature*, 424 (6950) (2003), pp. 810–816.
60. M.D. Wang et al., *Biophysical Journal*, 72 (3) (1997), pp. 1335–1346.
61. *Standard Test Methods for Tension Testing of Metallic Materials* (West Conshohocken, PA: ASTM, 2004).
62. W.N. Sharpe, *NASA Technical Memorandum (1989),* p. 101638.
63. Haibo Huang and F. Spaepen, *Acta Materialia*, 48 (12) (2000), pp. 3261–3269.
64. K.J. Hemker, B.G. Mendis, and C. Eberl, *Materials Science and Engineering A-Structural Materials Prop-*

erties Microstructure and Processing, 483 (2008), pp. 727–730.
65. D.S. Gianola et al., *Advanced Materials*, 20 (2008), pp. 303–308.
66. Nicholas Biery, Marc deGraef, and Tresa Pollock, *Metallurgical and Materials Transactions A*, 34 (10) (2003), pp. 2301–2313.
67. M. Sutton et al., *Experimental Mechanics*, 47 (6) (2007), pp. 775–787.
68. M. Sutton et al., *Experimental Mechanics*, 47 (6) (2007), pp. 789–804.
69. C. Eberl, D.S. Gianola, and R. Thompson, *MatLab Central* (Natick, MA: The Mathworks, Inc., 2006), File ID:12413.
70. J.J. Vlassak and W.D. Nix, *JMR*, 7 (1992), pp. 3242–3249.
71. H.D. Espinosa, B.C. Prorok, and B. Peng, *Journal of the Mechanics and Physics of Solids*, 52 (3) (2004), pp. 667–689.
72. N. André et al., *Microelectronic Engineering*, 84 (11) (2007), pp. 2714–2718.
73. M. Hommel and O. Kraft, *Acta Materialia*, 49 (19) (2001), pp. 3935–3947.
74. F. Macionczyk and W. Bruckner, *Journal of Applied Physics*, 86 (9) (1999), pp. 4922–4929.
75. Z. Suo et al., *Applied Physics Letters*, 87 (16) (2005), pp. 1–3.
76. N.S. Lu et al., *Applied Physics Letters*, 91 (22) (2007), p. 221909.
77. M.R. Begley and H. Bart-Smith, *International Journal of Solids and Structures*, 42 (18-19) (2005), pp. 5259–5273.
78. J. Bohm et al., *Review of Scientific Instruments*, 75 (4) (2004), pp. 1110–1119.
79. U. Welzel et al., *Journal of Applied Crystallography*, 38 (1) (2005), pp. 1–29.
80. P.A. Gruber et al., *JMR*, 23 (2008), pp. 2406–2419.
81. Patric A. Gruber et al., *Acta Materialia*, 56 (8) (2008), pp. 1876–1889.
82. Sven Olliges et al., *Acta Materialia*, 55 (15) (2007), pp. 5201–5210.
83. Y. Xiang and J.J. Vlassak, *Acta Materialia*, 54 (20) (2006), pp. 5449–5460.
84. L. Nicola et al., *J. Mechanics and Physics of Solids*, 54 (10) (2006), pp. 2089–2110.
85. B.C. Prorok, H.D. Espinosa, and M.A. Fischer, *J. Mechanics and Physics of Solids*, 51 (2003), pp. 41–67.
86. Autumn Kellar et al., *Nature*, 405 (6787) (2000), pp. 681–685.
87. Autumn Kellar et al., *Proceedings of the National Academy of Sciences of the United States of America*, 99 (19) (2002), pp. 12252–12256.
88. Gerrit Huber et al., *Proceedings of the National Academy of Sciences of the United States of America*, 102 (45) (2005), pp. 16293–16296.
89. Gerrit Huber et al., *Acta Biomaterialia*, 3 (4) (2007), pp. 607–610.
90. Ralph Spolenak, Stanislav Gorb, and Eduard Arzt, *Acta Biomaterialia*, 1 (1) (2005), pp. 5–13.
91. Christian Greiner, Ralph Spolenak, and Eduard Arzt, *Acta Biomaterialia*, 5 (2) (2009), pp. 597–606..
92. S.S. Brenner, *J. Applied Physics*, 27 (12) (1956), pp. 1484–1491.
93. S.S. Brenner, *J. Applied Physics*, 28 (9) (1957), pp. 1023–1026.
94. S.S. Brenner, *J. Applied Physics*, 30 (12) (1958), pp. 266–267.
95. P.M. Duxburry, *Statistical Models for the Fracture of Disordered Media* (St. Louis, MO: North-Holland Publishers, 1990), p. 189.
96. Michael D. Uchic et al., *Science*, 305 (5686) (2004), pp. 986–989.
97. Michael D. Uchic and Dennis M. Dimiduk, *Materials Science and Engineering A*, 400-401 (1-2 SUPPL) (2005), pp. 268–278.
98. Z.W. Shan et al., *Nat. Mater.*, 7 (2) (2008), pp. 115–119.
99. C.A. Volkert and E.T. Lilleodden, *Philosophical Magazine*, 86 (33) (2006), pp. 5567–5579.
100. C.P. Frick et al., *Materials Science and Engineering: A*, 489 (1-2) (2008), pp. 319–329.
101. J.R. Greer, W.C. Oliver, and W.D. Nix, *Acta Materialia,* 53 (6) (2005), pp. 1821–1830; "Erratum," *Acta Materialia*, 54 (6) (2006), p. 1705.
102. Julia R. Greer, Warren C. Oliver, and William D. Nix, *Acta Materialia*, 53 (6) (2005), pp. 1821–1830.
103. M. Zaiser et al., *Philosophical Magazine*, 8 (30) (2008), pp. 3861–3874.
104. Steffen Brinckmann, Ju-Young Kim, and Julia R. Greer, *Physical Review Letters*, 100 (15) (2008), p. 155502.
105. B.E. Schuster et al., *Acta Materialia*, 56 (18) (2008), pp. 5091–5100.
106. Z.W. Shan et al., *Physical Review B (Condensed Matter and Materials Physics)*, 77 (15) (2008), p. 155419.
107. C.A. Volkert, A. Donohue, and F. Spaepen, *J. Applied Physics*, 103 (8) (2008), p. 083539.
108. D.M. Dimiduk, M.D. Uchic, and T.A. Parthasarathy, *Acta Materialia*, 53 (15) (2005), pp. 4065–4077.
109. J.R. Greer and W.D. Nix, *Physical Review B (Condensed Matter and Materials Physics)*, 73 (24) (2006), p. 245410.
110. D. Kiener, W. Grosinger, and G. Dehm, *Scripta Materialia*, 60 (3) (2009), pp. 148–151.
111. D. Kiener et al., *Acta Materialia*, 56 (3) (2008), pp. 580–592.
112. H. Bei et al., *Scripta Materialia*, 57 (5) (2007), pp. 397–400.
113. H. Bei et al., *Applied Physics Letters*, 91 (11) (2007), p. 111915.
114. H. Bei et al., *Acta Materialia*, 56 (17) (2008), pp. 4762–4770.
115. K.S. Kumar, H. Van Swygenhoven, and S. Suresh, *Acta Materialia*, 51 (19) (2003), pp. 5743–5774.
116. M.W. Chen, E. Ma, and K.J. Hemker, *Nanomaterials Handbook,* ed. Yury Gogotsi (Boca Raton, FL: CRC Press, 2006), pp. 497–531.
117. D. Wolf et al., *Acta Materialia*, 53 (1) (2005), pp. 1–40.
118. M. Legros et al., *Philosophical Magazine A: Physics of Condensed Matter, Structure, Defects and Mechanical Properties*, 80 (4) (2000), pp. 1017–1026.
119. Zeljka Budrovic et al., *Science*, 304 (5668) (2004), pp. 273–276.
120. D. Pan et al., *Scripta Materialia*, 48 (12) (2003), pp. 1581–1586.
121. D.S. Gianola et al., *Scripta Materialia*, 55 (7) (2006), pp. 649–652.
122. D.S. Gianola et al., *Materials Science and Engineering: A*, 483-484 (2008), pp. 637–640.
123. G. Gottstein and L.S. Shvindlerman, *Grain Boundary Migration in Metals Thermodynamics, Kinetics, Applications* (Boca Raton, FL: CRC Press, 1999).
124. J.W. Cahn and J.E. Taylor, *Acta Materialia*, 52 (16) (2004), pp. 4887–4898.
125. J.W. Cahn, Y. Mishin, and A. Suzuki, *Acta Materialia*, 54 (19) (2006), pp. 4953–4975.
126. M. Ashby and D.R.H. Jones, *Engineering Materials 1: An Introduction to Properties, Applications and Design*, 3rd edition (St. Louis, MO: Butterworth-Heinemann, 2005).
127. D.T. Read, *International Journal of Fatigue*, 20 (3) (1998), pp. 203–209.
128. G.P. Zhang et al., *Microelectronics Reliability*, 47 (12) (2007), pp. 2007–2013.
129. Jun-Hyub Park, ManSik Myung, and Yun-Jae Kim, *Sensors and Actuators A: Physical*, 147 (2) (2008), pp. 561–569.
130. M.A. Eby, W.M. Sharpe, Jr., and G. Coles, *Proceedings Transducers '01* (Berlin: Springer-Verlag, 2001), pp. 1366–1369.

D.S. Gianola and C. Eberl are with Karlsruhe Institute of Technology, Karlsruhe, Germany and can be reached at Dan.Gianola@kit.edu, Chris.Eberl@kit.edu